

Accepted Manuscript

Research paper

Syntheses, structures, and inhibition studies of *Jack bean* urease by copper(II) complexes derived from a tridentate hydrazone ligand

Zhonglu You, Huiyuan Yu, Boyang Zheng, Chenglu Zhang, Chengwei Lv, Kun Li, Lin Pan

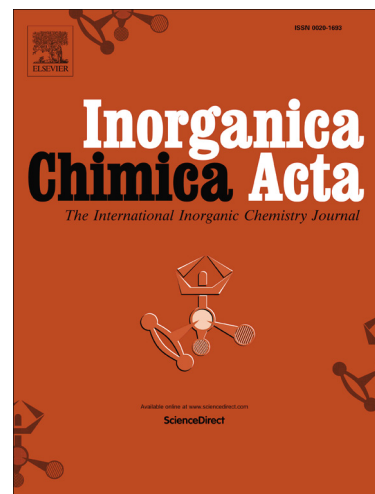
PII: S0020-1693(17)31232-X
DOI: <http://dx.doi.org/10.1016/j.ica.2017.09.011>
Reference: ICA 17867

To appear in: *Inorganica Chimica Acta*

Received Date: 7 August 2017
Revised Date: 5 September 2017
Accepted Date: 5 September 2017

Please cite this article as: Z. You, H. Yu, B. Zheng, C. Zhang, C. Lv, K. Li, L. Pan, Syntheses, structures, and inhibition studies of *Jack bean* urease by copper(II) complexes derived from a tridentate hydrazone ligand, *Inorganica Chimica Acta* (2017), doi: <http://dx.doi.org/10.1016/j.ica.2017.09.011>

This is a PDF file of an unedited manuscript that has been accepted for publication. As a service to our customers we are providing this early version of the manuscript. The manuscript will undergo copyediting, typesetting, and review of the resulting proof before it is published in its final form. Please note that during the production process errors may be discovered which could affect the content, and all legal disclaimers that apply to the journal pertain.



Syntheses, structures, and inhibition studies of *Jack bean* urease by copper(II) complexes derived from a tridentate hydrazone ligand

Zhonglu You*, Huiyuan Yu, Boyang Zheng, Chenglu Zhang, Chengwei Lv, Kun Li,
Lin Pan

*Department of Chemistry and Chemical Engineering, Liaoning Normal University,
Dalian 116029, P. R. China*

ABSTRACT

Urease inhibitors can counteract the negative effects of urease. In this paper, three new copper(II) complexes derived from 3-methyl-*N'*-(pyridin-2-ylmethylene)benzohydrazide (HL) were prepared. They are [CuBr(CH₃OH)L] (**1**), [Cu(CH₃OH)L(NCS)] (**2**), and [CuL(HL)]·ClO₄ (**3**). The complexes were characterized by infrared and UV-Vis spectra, and single crystal X-ray determination. The Cu atoms in complexes **1** and **2** display square pyramidal coordination, and in complex **3** the Cu atom displays octahedral coordination. Complex **1** shows effective urease inhibitory activity, with IC₅₀ value of 1.46 ± 0.83 μM. Molecular docking study of the complexes with *Jack bean* urease was performed.

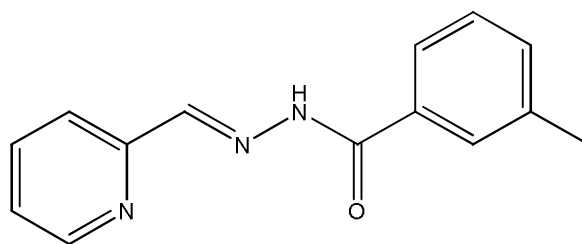
Keywords: Hydrazone; Copper complex; Crystal structure; Urease inhibition; Molecular docking

1. Introduction

* Corresponding author. Zhonglu You, Department of Chemistry and Chemical Engineering, Liaoning Normal University, Dalian 116029, P. R. China. Tel.: +8641182156989. Fax.: +8641182159660. E-mail address: youzhonglu@126.com

Urease (E.C.3.5.1.5) plays an important role in plant nitrogen metabolism [1-3]. However, excessive levels of urease in soil can degrade the fertilizer urea quickly, and result in phytopathic effects and loss of ammonia [4]. Moreover, urease is regarded as a virulent factor in human and animal infections of the urinary and gastrointestinal tracts [5]. Studies indicated that control of the activity of urease through the use of inhibitors could counteract the negative effects [6-14].

Metal complexes are well established enzyme inhibitors [15]. In recent years, we have reported a number of metal complexes with urease inhibitory activities [16-20]. Among the compounds, copper(II) complexes have the most effective urease inhibitory activities. Li and coworkers have reported some Schiff base copper(II) complexes with potent urease inhibitory activities [21,22]. However, the relationship between structures and urease inhibitory activities is not clear. Hydrazone is a kind of special Schiff base, which possess the typical functional group $-\text{CH}=\text{N}-\text{NH}-\text{C}(\text{O})-$. It has been shown that hydrazones have interesting biological activities, including urease inhibitory activity [23]. In this paper, three new copper(II) complexes, $[\text{CuBr}(\text{CH}_3\text{OH})\text{L}]$ (**1**), $[\text{Cu}(\text{CH}_3\text{OH})\text{L}(\text{NCS})]$ (**2**), and $[\text{CuL}(\text{HL})]\cdot\text{ClO}_4$ (**3**), where L is the monoanionic form of 3-methyl-*N'*-(pyridin-2-ylmethylene)benzohydrazide (HL), were synthesized and structurally characterized. The urease inhibitory activity of the complexes was investigated both from experimental and molecular docking analysis.



HL

2. Experimental section

2.1. Materials and measurements

Starting materials, reagents and solvents were purchased from commercial suppliers with AR grade, and used without purification. Elemental analyses were performed on a Perkin-Elmer 240C elemental analyzer. IR spectra were recorded on a Jasco FT/IR-4000 spectrometer as KBr pellets in the 4000–400 cm^{-1} region. UV-Vis spectra were recorded on a Perkin-Elmer Lambda 900 spectrometer. The urease inhibitory activity was measured on a Bio-Tek Synergy HT microplate reader. Single crystal structures were determined by Bruker D8 Venture single crystal diffraction.

2.2. Synthesis of HL

Pyridine-2-carboxaldehyde (1.0 mmol, 0.107 g) and 3-methylbenzohydrazide (1.0 mmol, 0.150 g) were dissolved in methanol (30 mL). The mixture was stirred at room temperature for 1 h to give a clear solution. The solvent was evaporated to give colorless solid product, which was re-crystallized from methanol. Yield: 212 mg (89%). Characteristic IR data (KBr, cm^{-1}): 3453 (OH), 1617 (CH=N). Anal. Calcd for $\text{C}_{14}\text{H}_{13}\text{N}_3\text{O}$: C, 70.3; H, 5.5; N, 17.6. Found: C, 70.1; H, 5.5; N, 17.5%. ^1H NMR (d^6 -DMSO): δ : 2.33 (s, 3H, CH_3), 7.35–7.90 (m, 8H, ArH), 8.71 (d, 1H, ArH), 11.82 (s, 1H, NH).

2.3. Synthesis of the complexes

[CuBr(CH₃OH)L] (1)

The hydrazone HL (1.0 mmol, 0.239 g) was dissolved in methanol (15 mL), to which was added dropwise CuBr_2 (1.0 mmol, 0.223 g) dissolved in methanol (10 mL). The mixture was magnetic stirred for 10 min at room temperature, and filtered. The filtrate was kept in air for a few days, to form crystals suitable for single crystal X-ray diffraction. The crystals were isolated, washed three times with cold methanol and dried in air. Yield: 175 mg (42%). Characteristic IR data (KBr, cm^{-1}): 3441 (OH),

1603 (CH=N). UV-Vis data [methanol, λ/nm ($\epsilon/\text{L}\cdot\text{mol}^{-1}\cdot\text{cm}^{-1}$): 272 (5,850), 380 (7,980), 657 (110). Anal. Calcd for $\text{C}_{15}\text{H}_{16}\text{BrCuN}_3\text{O}_2$: C, 43.5; H, 3.9; N, 10.2. Found: C, 43.7; H, 4.0; N, 10.0%. A_M (10^{-3} M in acetonitrile): $21 \Omega^{-1}\cdot\text{cm}^2\cdot\text{mol}^{-1}$.

[Cu(CH₃OH)L(NCS)] (2)

The hydrazone HL (1.0 mmol, 0.239 g) was dissolved in methanol (15 mL), to which was added dropwise CuBr₂ (1.0 mmol, 0.223 g) and ammonium thiocyanate (1.0 mmol, 0.076 g) dissolved in methanol (15 mL). The mixture was magnetic stirred for 10 min at room temperature, and filtered. The filtrate was kept in air for a few days, to form crystals suitable for single crystal X-ray diffraction. The crystals were isolated, washed three times with cold methanol and dried in air. Yield: 203 mg (52%). Characteristic IR data (KBr, cm^{-1}): 3450 (OH), 2093 (NCS), 1604 (CH=N). UV-Vis data [methanol, λ/nm ($\epsilon/\text{L}\cdot\text{mol}^{-1}\cdot\text{cm}^{-1}$): 269 (4,450), 392 (15,270), 646 (125). Anal. Calcd for $\text{C}_{16}\text{H}_{16}\text{CuN}_4\text{O}_2\text{S}$: C, 49.0; H, 4.1; N, 14.3. Found: C, 48.9; H, 4.2; N, 14.3%. A_M (10^{-3} M in acetonitrile): $18 \Omega^{-1}\cdot\text{cm}^2\cdot\text{mol}^{-1}$.

[CuL(HL)]·ClO₄ (3)

The hydrazone HL (1.0 mmol, 0.239 g) was dissolved in methanol (15 mL), to which was added dropwise Cu(ClO₄)₂·7H₂O (1.0 mmol, 0.388 g) dissolved in methanol (15 mL). The mixture was magnetic stirred for 10 min at room temperature, and filtered. The filtrate was kept in air for a few days, to form crystals suitable for single crystal X-ray diffraction. The crystals were isolated, washed three times with cold methanol and dried in air. Yield: 231 mg (36%). Characteristic IR data (KBr, cm^{-1}): 3190 (NH), 1609 (CH=N), 1162 (ClO₄). UV-Vis data [methanol, λ/nm ($\epsilon/\text{L}\cdot\text{mol}^{-1}\cdot\text{cm}^{-1}$): 275 (5,135), 378 (8,230), 670 (143). Anal. Calcd for $\text{C}_{28}\text{H}_{25}\text{ClCuN}_6\text{O}_6$: C, 52.5; H, 3.9; N, 13.1. Found: C, 52.3; H, 4.1; N, 13.1%. A_M (10^{-3} M in acetonitrile): $135 \Omega^{-1}\cdot\text{cm}^2\cdot\text{mol}^{-1}$.

2.4. X-ray crystallography

Diffraction intensities for the complexes were collected at 298(2) K using a Bruker D8 Venture diffractometer with MoK α radiation ($\lambda = 0.71073 \text{ \AA}$). The collected data were reduced with SAINT [24], and multi-scan absorption correction was performed using SADABS [25]. Structures of the complexes were solved by direct methods and refined against F^2 by full-matrix least-squares method using SHELXTL [26]. All of the non-hydrogen atoms were refined anisotropically. The methanol H atoms in **1** and **2**, and the amino H atom in **3** were located from difference Fourier maps and refined isotropically, with O–H and N–H distances restrained to 0.85(1) and 0.90(1) \AA , respectively. The remaining hydrogen atoms were placed in calculated positions and constrained to ride on their parent atoms. Crystallographic data for the complexes are summarized in Table 1. Selected bond lengths and angles are given in Table 2.

2.5. Urease inhibitory activity assay

The measurement of urease inhibitory activity was carried out according to the literature method [27]. The assay mixture containing 75 μL of *Jack bean* urease and 75 μL of tested compounds with various concentrations (dissolved in DMSO) was pre-incubated for 15 min on a 96-well assay plate. Acetohydroxamic acid was used as a reference. Then 75 μL of phosphate buffer at pH 6.8 containing phenol red (0.18 mM) and urea (400 mM) were added and incubated at room temperature. The reaction time required for enough ammonium carbonate to form to raise the pH phosphate buffer from 6.8 to 7.7 was measured by micro-plate reader (560 nm) with end-point being determined by the color change of phenol-red indicator.

2.6. Inhibition kinetic study

The maximum velocity (v_{max}) values were determined by means of Lineweaver–Burk plots, using initial velocities obtained over substrate concentrations

of 41.4, 20.7, 10.35, and 5.17 $\mu\text{g}\cdot\text{mL}^{-1}$, respectively. Inhibitory constant (K_i) value was calculated from the Dixon plot. Alternatively, K_i value was determined from abscissa of the plots of slopes vs. different concentrations of the complex, in which slope was obtained from the Lineweaver–Burk lines [28].

2.7. Docking study

Molecular docking study of the complexes into the 3D X-ray structure of the *Jack bean* urease (entry 4UBP in the Protein Data Bank) was carried out by using the AutoDock 4.0 software as implemented through the graphical user interface AutoDockTools (ADT 1.5.2). The graphical user interface AutoDockTools was employed to setup the enzymes: all hydrogens were added, Gasteiger charges were calculated and nonpolar hydrogens were merged to carbon atoms. The Ni initial parameters are set as $r = 1.170 \text{ \AA}$, $q = +2.0$, and *van der Waals* well depth of $0.100 \text{ kcal}\cdot\text{mol}^{-1}$ [29]. The 3D structures of the ligand molecules were saved in pdb format with the aid of the program ChemBio3D. The resulting files were saved as pdbqt format.

The AutoDockTools was used to generate the docking input files. The maps were centered on the original ligand molecule, acetohydroxamic acid, in the catalytic site of the protein. A grid spacing of 0.375 \AA and a distances-dependent function of the dielectric constant were used for the calculation of the energetic map. 100 runs were generated by using Lamarckian genetic algorithm searches. Default settings were used with an initial population of 50 randomly placed individuals, a maximum number of 2.5×10^6 energy evaluations, and a maximum number of 2.7×10^4 generations. A mutation rate of 0.02 and a crossover rate of 0.8 were chosen. The results of the most favorable free energy of binding were selected as the resultant complex structures.

3. Results and discussion

3.1. Chemistry

The copper complexes were readily prepared by the reaction of equimolar quantities of the hydrazone ligand, copper salts, and/or secondary ligand (NCS) in methanol. Single crystals of the complexes were obtained by slow evaporation of the methanolic solution of the complexes. The hydrazone ligands in complexes **1** and **2** adopt enolate form, while those in complex **3** adopt both enolate and *keto* forms. The three complexes are stable in air at room temperature. Molar conductivities of complexes **1** and **2** measured in methanol at concentration of 10^{-3} M are about $20 \Omega^{-1} \text{ cm}^2 \text{ mol}^{-1}$, indicating the non-electrolytic nature of them in such solution [30]. Molar conductivity of complex **3** measured in methanol at concentration of 10^{-3} M is $135 \Omega^{-1} \text{ cm}^2 \text{ mol}^{-1}$, which indicates the 1:1 electrolytic nature [30].

3.2. Structure description of the complexes

Structure description of **1**

Molecular structure of complex **1** is shown in Figure 1. The Cu atom in the complex is in square pyramidal geometry, with the pyridine N, imino N and enolate O atoms of the hydrazone ligand, and the Br atom located at the basal plane, and with the methanol O atom located at the apical position. The Cu atom deviates from the least-squares plane defined by the four basal donor atoms by $0.212(1) \text{ \AA}$. The coordinate bond lengths in the complex are comparable to those observed in copper(II) complexes with hydrazone ligands [31,32]. The distortion of the square pyramidal geometry can be observed from the deviation of the coordinate bond angles from the ideal square pyramid (Table 2), which are caused by the strain created from the five-membered chelate rings Cu1-N1-C5-C6-N2 and Cu1-N2-N3-C7-O1. The dihedral angle between the pyridine and the benzene rings of the hydrazone ligand is $3.1(3)^\circ$.

In the crystal structure of the complex, molecules are linked by methanol ligands through intermolecular hydrogen bonds (Table 3), to form dimers (Figure 2).

Structure description of complex **2**

Molecular structure of complex **2** is shown in Figure 3. The Cu atom in the complex is in square pyramidal geometry, with the pyridine N, imino N and enolate O atoms of the hydrazone ligand, and the N atom of the thiocyanate ligand located at the basal plane, and with the methanol O atom located at the apical position. The Cu atom deviates from the least-squares plane defined by the four basal donor atoms by 0.118(1) Å. The coordinate bond lengths in the complex are similar to complex **1** and also comparable to those observed in copper(II) complexes with hydrazone ligands [31,32]. The distortion of the square pyramidal geometry can be observed from the deviation of the coordinate bond angles from the ideal square pyramid (Table 2), which are caused by the strain created from the five-membered chelate rings Cu1-N1-C5-C6-N2 and Cu1-N2-N3-C7-O1. The dihedral angle between the pyridine and the benzene rings of the hydrazone ligand is 15.6(4)°.

In the crystal structure of the complex, molecules are linked by methanol ligands through intermolecular hydrogen bonds (Table 3), to form dimers (Figure 4).

Structure description of complex **3**

Molecular structure of complex **3** is shown in Figure 5. The asymmetric unit of the complex contains a mononuclear copper(II) complex cation and a perchlorate anion. The Cu atom is coordinated in an octahedral geometry by two hydrazone ligands, one adopts monoanionic enolate form, and the other one adopts neutral *keto* form. It is clear that the coordinate bond lengths of the neutral hydrazone ligand are longer than the corresponding bonds in the monoanionic hydrazone ligand. Thus, the equatorial plane of the octahedral geometry can be defined by the three donor atoms (O2, N5,

N4) of the monoanionic hydrazone ligand, and the imino N atom (N2) of the neutral hydrazone ligand, and the apical positions can be defined by the remaining two donor atoms of the neutral hydrazone ligand. The Cu atom deviates from the least-squares plane defined by the equatorial donor atoms by 0.041(1) Å. The distortion of the octahedral geometry can be observed from the deviation of the coordinate bond angles from the ideal values (Table 2).

In the crystal structure of the complex, molecules are linked by intermolecular hydrogen bonds (Table 3), to form chains along the *a* axis (Figure 6).

3.3. IR and UV-Vis spectra

The medium and broad absorption centered at about 3450 cm⁻¹ in the spectra of complexes **1** and **2** substantiate the presence of O–H groups. The sharp bands indicative of the N–H vibration of complex **3** is located at 3190 cm⁻¹. The strong absorption bands in the region 1600–1610 cm⁻¹ for the complexes are assigned to the azomethine $\nu(\text{C}=\text{N})$ [33]. The intense absorption at 2093 cm⁻¹ for complex **2** can be assigned to the vibration of the NCS ligand [34]. The band indicative of the perchlorate anion in complex **3** is observed at 1162 cm⁻¹.

Electronic spectra of the complexes were recorded in methanol with concentration of 10⁻⁵ M. The complexes displayed strong bands centered at about 270 nm, which can be assigned to the intra-ligand $\pi-\pi^*$ transition of the aromatic rings. The charge transfer LMCT bands are located in the range 370–390 nm. The spectra showed weak and broad *d-d* electronic transitions in the range 640–670 nm, which are assigned to ${}^2\text{E}_{\text{g}(\text{D})} \rightarrow {}^2\text{T}_{2\text{g}(\text{D})}$ [35].

3.4. Pharmacology study

The percent inhibition of the complexes at concentration of 12.5 μM on *Jack bean* urease and IC₅₀ values are listed in Table 4. Complex **1** shows excellent urease

inhibitory activity with IC_{50} value of $1.46 \pm 0.83 \mu\text{M}$. Complexes **2** and **3** show from medium to strong activities with IC_{50} values of 10.8 ± 2.1 and $15.4 \pm 1.8 \mu\text{M}$, respectively. As a comparison, AHA was used as a reference with the percent inhibition of 64.0 ± 2.7 , and with IC_{50} value of $36.3 \pm 2.5 \mu\text{M}$. Copper perchlorate can inhibit urease activity, with IC_{50} value of $8.5 \pm 1.7 \mu\text{M}$. The present copper complexes have stronger activities than the copper(II) complex with *N*-hydroxyethyl-*N*-benzimidazolymethylethylenediaminediacetic acid ($IC_{50} = 35 \mu\text{M}$) [36], and also stronger than the copper(II) complexes with Schiff base ligands ($IC_{50} = 19$ and $39 \mu\text{M}$) [37]. However, the complexes have a little weak activity than the copper(II) complexes with hydrazone ligands derived from salicylaldehyde and its analogues [38].

3.5. Kinetic study of the urease inhibitory activity by complex **1**

Complex **1** has the most effective urease inhibitory activity. Thus, the inhibition mechanism of the complex was studied with Lineweaver-Burk plots (Figure 7a). The type of inhibition was elucidated from analysis of Lineweaver-Burk plots. For Lineweaver-Burk plot, the slope of the resulting line is K_m/v_{max} , the y -intercept is $1/v_{\text{max}}$, and the x -intercept is $1/K_m$. The figure shows a series of lines intersect one with another in the third quadrant while the y -intercept of the plots increased with the increase of the concentration ($5.17, 10.35, 20.7, 41.4 \mu\text{g}\cdot\text{mL}^{-1}$) of the complex. This illustrated the inhibition of the urease by the complex caused a decrease in v_{max} with change of K_m values, suggesting a mixed-competitive inhibition type. The K_i value of -4.5 was calculated from the slope of the Lineweaver-Burk plot vs. the concentration of inhibitor (Figure 7b).

3.6. Molecular docking study

Molecular docking study was performed to investigate the binding effects between

the molecules of the complexes and the active site of the *Jack bean* urease. The binding models of complexes **1**, **2** and **3** with the urease were depicted in Figures 8-10, respectively. The results revealed that the molecule of complex **1** fits well with the active pocket of the urease, while complexes **2** and **3** cannot enter the active pocket. The size of the molecules might be the basal principle of the inhibition. Additional interactions have been established in a variety of conformations because of the flexibility of the complex molecules and the amino acid residues of the enzyme. The optimized clusters (100 occurrences each) were ranked by energy level in the best conformation of inhibitor–urease modeled structures, where the docking scores are -5.98 (**1**), -5.83 (**2**), and -7.88 (**3**), respectively. As a comparison, the docking score for the AHA inhibited model is -5.01 . The negative values indicate that the complex molecules bind well with the urease.

The mechanism of urease inhibition by complex **1** was considered to be embedded in the active pocket of the urease and interact with the residues MET366, HIS322, ALA365 and GLN364. The Br ligand of complex **1** is close to the Ni atom of the enzyme. In addition, there are some hydrophobic interactions between the complex and the residues of the urease. The mechanism of urease inhibition by complexes **2** and **3** was considered to be partial blockage of the entrance of the urease active pocket, which hindered the urea to access to the urease active center.

4. Conclusion

The present study reports the syntheses, characterization and crystal structures of three new copper(II) complexes with 3-methyl-*N'*-(pyridin-2-ylmethylene)benzohydrazide as ligand. Complex **1** shows excellent urease inhibitory activity, with IC_{50} value of $1.46 \pm 0.83 \mu\text{M}$. The complex

has a mixed competitive inhibition mechanism. Molecular docking study indicated that suitable size and conformations of the complexes are required for the inhibition of the urease. The biological evaluation and mechanism study of the compounds reveal that complex **1** is a prospective urease inhibitor.

Supplementary data

CCDC 1553134 (**1**), 1553135 (**2**) and 1553157 (**3**) contain the supplementary crystallographic data for this paper. These data can be obtained free of charge *via* <http://www.ccdc.cam.ac.uk/conts/retrieving.html>, or from the Cambridge Crystallographic Data Centre, 12 Union Road, Cambridge CB2 1EZ, UK; fax: (+44) 1223-336-033; or e-mail: deposit@ccdc.cam.ac.uk.

Acknowledgments

This work was financially supported by the Natural Science Foundation of China (Project No. 21641012).

References

- [1] S. Cruchaga, B. Lasa, I. Jauregui, C. Gonzalez-Murua, P.M. Aparicio-Tejo, I. Ariz, *Plant Soil* 373 (2013) 813-827.
- [2] P.A. Karplus, M.A. Pearson, R.P. Hausinger, *Acc. Chem. Res.* 30 (1997) 330-337.
- [3] J.B. Sumner, *J. Biol. Chem.* 69 (1926) 435-441.
- [4] J.R. Soares, H. Cantarella, M.L.D. Menegale, *Soil Biol. Biochem.* 52 (2012) 82-89.
- [5] M. Perrais, C. Rousseaux, M.P. Ducourouble, R. Courcol, P. Vincent, N. Jonckheere, I. Van Seuningem, *Gastric Cancer* 17 (2014) 235-246.
- [6] L.V. Modolo, A.X. de Souza, L.P. Horta, D.P. Araujo, A. de Fatima, *J. Adv. Res.* 6 (2015) 35-44.

- [7] Z.-P. Xiao, Z.-Y. Peng, J.-J. Dong, R.-C. Deng, X.-D. Wang, H. Ouyang, P. Yang, J. He, Y.-F. Wang, M. Zhu, *Eur. J. Med. Chem.* 68 (2013) 212-221.
- [8] T.G. Barros, J.S. Williamson, O.A.C. Antunes, E.M.F. Muri, *Lett. Drug Des. Discov.* 6 (2009) 186-192.
- [9] Zaheer-Ul-Haq, A. Wadood, R. Uddin, *J. Enzyme Inhib. Med. Chem.* 24 (2009) 272-278.
- [10] K.F. Bronson, A.R. Mosier, *Biol. Fert. Soils* 17 (1994) 263-268.
- [11] K.R.C. Reddy, A.M. Kayastha, *J. Enzyme Inhib. Med. Chem.* 21 (2006) 467-470.
- [12] S. Kumar, A.M. Kayastha, *J. Enzyme Inhib. Med. Chem.* 25 (2010) 646-652.
- [13] W. Zaborska, B. Krajewska, Z. Olech, *J. Enzym. Inhib. Med. Chem.* 19 (2004) 65-69.
- [14] W. Zaborska, B. Krajewska, M. Leszko, Z. Olech, *J. Mol. Catal. B: Enzym.* 13 (2001) 103-108.
- [15] A.Y. Louie, T.J. Meade, *Chem. Rev.* 99 (1999) 2711-2734.
- [16] D. Qu, F. Niu, X. Zhao, K.-X. Yan, Y.-T. Ye, J. Wang, M. Zhang, Z. You, *Bioorg. Med. Chem.* 23 (2015) 1944-1949.
- [17] Z.-L. You, L. Zhang, D.-H. Shi, X.-L. Wang, X.-F. Li and Y.-P. Ma, *Inorg. Chem. Commun.* 13 (2010) 996-998.
- [18] Z.-L. You, D.-H. Shi, J.-C. Zhang, Y.-P. Ma, C. Wang, K. Li, *Inorg. Chim. Acta* 384 (2012) 54-61.
- [19] Z.-L. You, Y. Lu, N. Zhang, B.-W. Ding, H. Sun, P. Hou, C. Wang, *Polyhedron* 30 (2011) 2186-2194.
- [20] Z.-L. You, L.-L. Ni, D.-H. Shi, S. Bai, *Eur. J. Med. Chem.* 45 (2010) 3196-3199.
- [21] X.-W. Dong, T.-L. Guo, Y.-G. Li, Y.-M. Cui, Q. Wang, *J. Inorg. Biochem.* 127 (2013) 82-89.

- [22] Y.-M. Cui, X.-W. Dong, W. Chen, W.-J. Wang, Y.-G. Li, H.-L. Zhu, J. Enzyme Inhib. Med. Chem. 27 (2012) 528-532.
- [23] M. Taha, N.H. Ismail, M.S. Baharudin, S. Lalani, S. Mehboob, K.M. Khan, S. yousuf, S. Siddiqui, F. Rahim, M.I. Choudhary, Med. Chem. Res. 24 (2015) 1310-1324.
- [24] Bruker, SMART (Version 5.628) and SAINT (Version 6.02); Bruker AXS: Madison, Wisconsin, USA, 1998.
- [25] G.M. Sheldrick, SADABS Program for Empirical Absorption Correction of Area Detector; University of Göttingen: Germany, 1996.
- [26] G.M. Sheldrick, Acta Crystallogr. A64 (2008) 112-122.
- [27] T. Tanaka, M. Kawase, S. Tani, Life Sci. 73 (2003) 2985-2990.
- [28] Z. Amtul, M. Rasheed, M.I. Choudhary, R. Supino, K.M. Khan, R. Atta Ur, Biochem. Biophys. Res. Commun. 319 (2004) 1053-1063.
- [29] B. Krajewska, W. Zaborska, Bioorg. Chem. 35 (2007) 355-365.
- [30] W.J. Geary, Coord. Chem. Rev. 7 (1971) 81-122.
- [31] L.-M. Wu, H.-B. Teng, X.-C. Feng, X.-B. Ke, Q.-F. Zhu, J.-T. Su, W.-J. Xu, X.-M. Hu, Cryst. Growth Des. 7 (2007) 1337-1342.
- [32] M.F. Iskander, T.E. Khalil, R. Werner, W. Haase, I. Svoboda, H. Fues, Polyhedron 19 (2000) 1181-1191.
- [33] Z.-L. You, M. Zhang, D.-M. Xian, Dalton Trans. 41 (2012) 2515-2524.
- [34] Z.-L. You, D.-M. Xian, M. Zhang, CrystEngComm 14 (2012) 7133-7136.
- [35] A.A. Alhadi, S.A. Shaker, W.A. Yehye, H.M. Ali, M.A. Abdullah, Bull. Chem. Soc. Ethiopia 25 (2012) 95-101.
- [36] L. Habala, A. Roller, M. Matuska, J. Valentova, A. Rompel, F. Devinsky, Inorg. Chim. Acta 421 (2014) 423-426.

[37] Y. Gou, M. Yu, Y. Li, Y. Peng, W. Chen, *Inorg. Chim. Acta* 404 (2013) 224-229.

[38] L. Pan, C. Wang, K. Yan, K. Zhao, G. Sheng, H. Zhu, X. Zhao, D. Qu, F. Niu, Z.

You, J. *Inorg. Biochem.* 159 (2016) 22-28.

ACCEPTED MANUSCRIPT

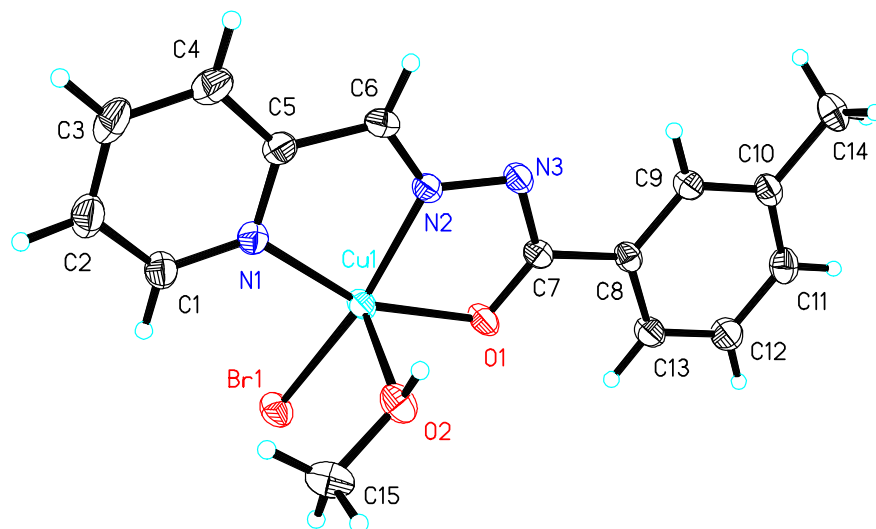


Figure 1. Molecular structure of **1**, showing the atom-numbering scheme. Displacement ellipsoids are drawn at the 30% probability level and H atoms are shown as small spheres of arbitrary radii.

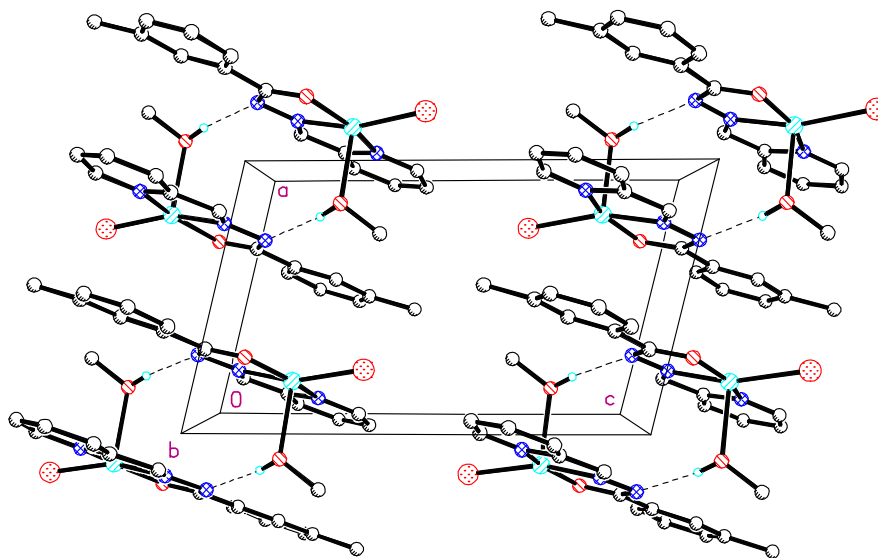


Figure 2. Molecular packing diagram of **1**, viewed along the *b* axis. Hydrogen bonds are shown as dashed lines.

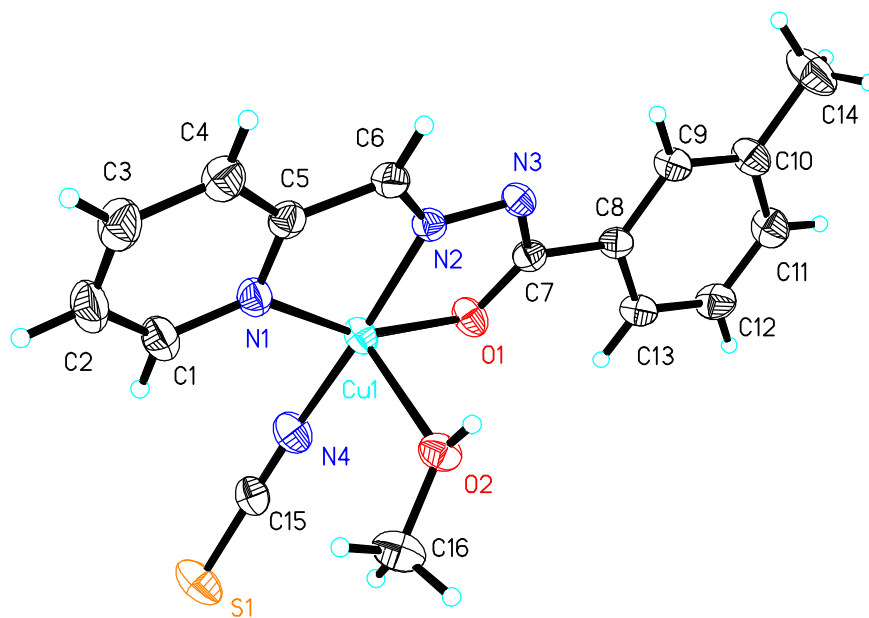


Figure 3. Molecular structure of **2**, showing the atom-numbering scheme. Displacement ellipsoids are drawn at the 30% probability level and H atoms are shown as small spheres of arbitrary radii.

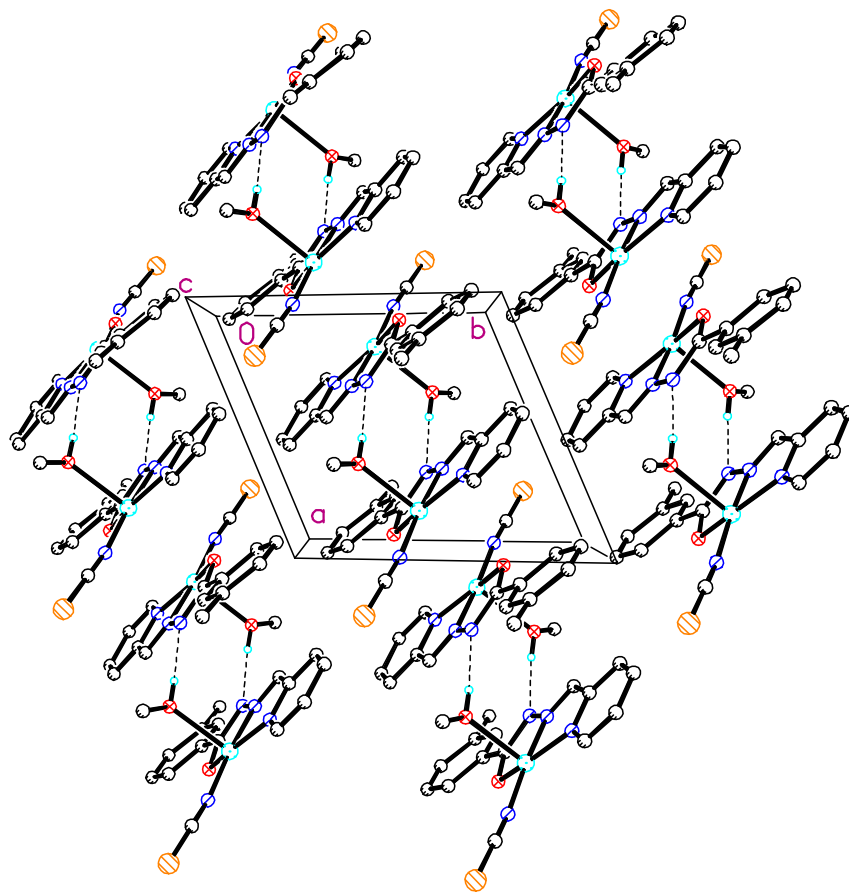


Figure 4. Molecular packing diagram of **2**, viewed along the *c* axis. Hydrogen bonds are shown as dashed lines.

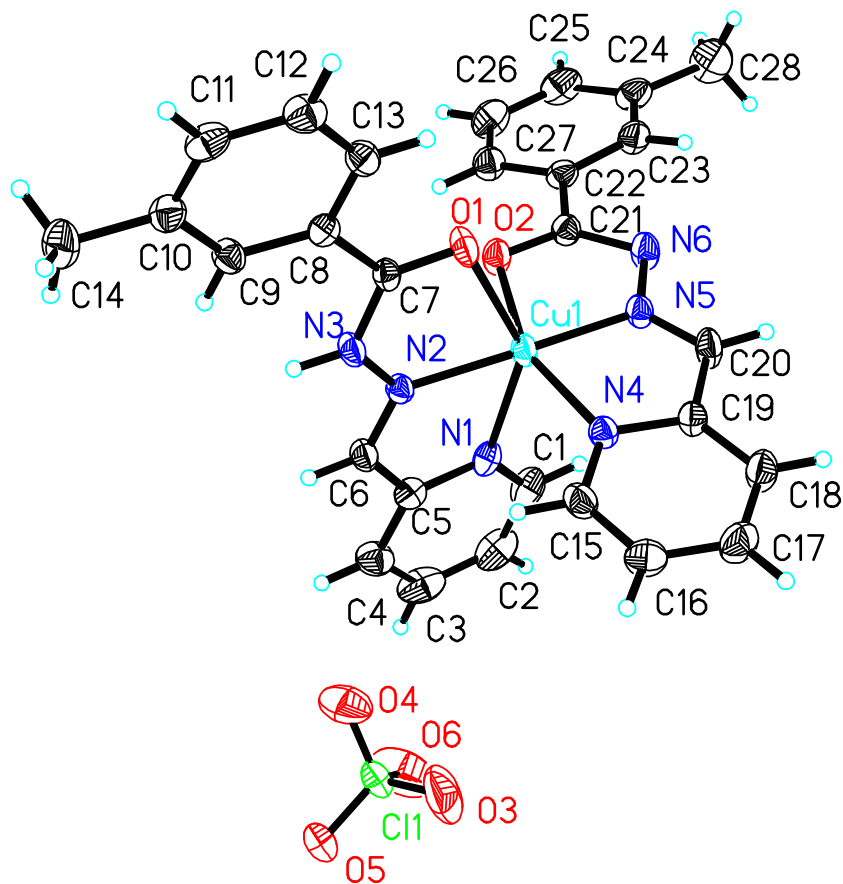


Figure 5. Molecular structure of **3**, showing the atom-numbering scheme. Displacement ellipsoids are drawn at the 30% probability level and H atoms are shown as small spheres of arbitrary radii.

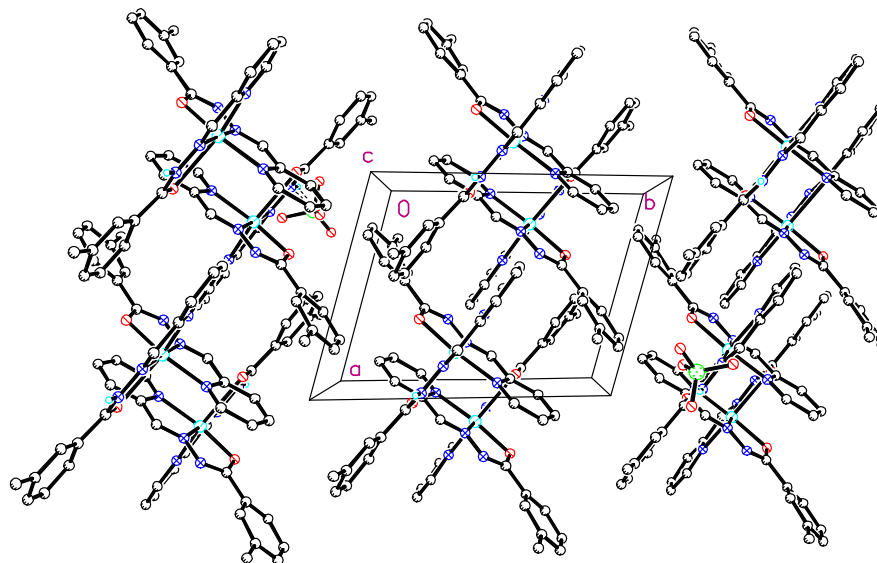


Figure 6. Molecular packing diagram of **3**, viewed along the *c* axis. Hydrogen bonds are shown as dashed lines.

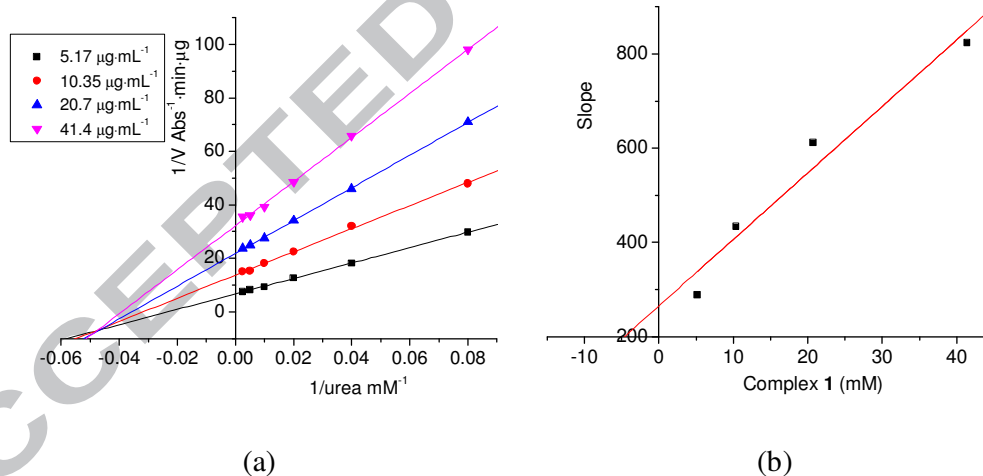


Figure 7. (a) Lineweaver–Burk plot of the reciprocal of initial velocities *vs.* the reciprocal of substrate concentration in the presence of 41.4, 20.7, 10.35, and 5.17 μM of complex **1**. (b) Plot of the slopes from the Lineweaver-Burk plots *vs.* various concentrations of complex **1**.

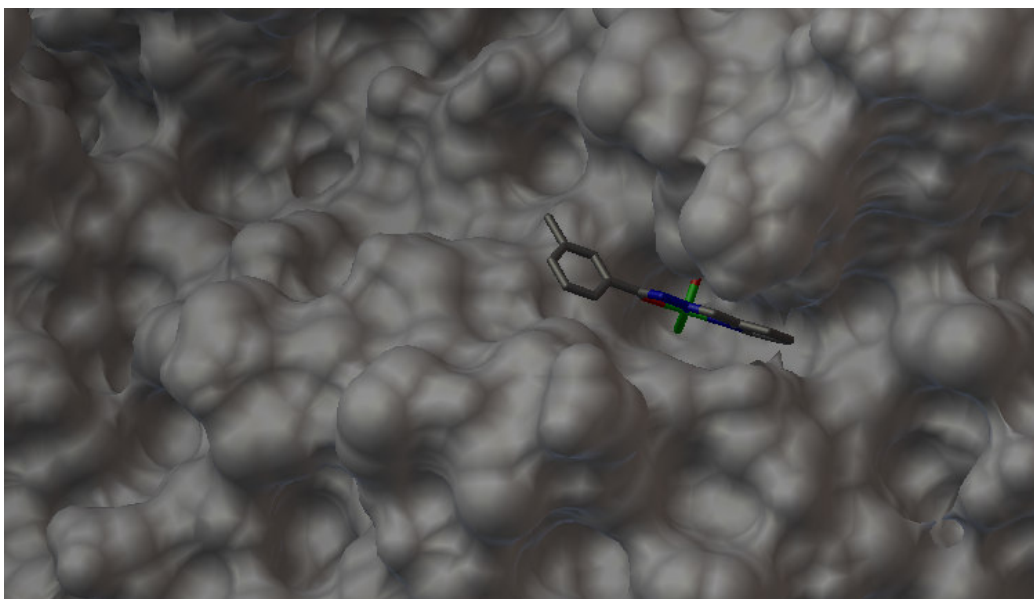


Figure 8a. Binding mode of **1** with *Jack bean* urease. The enzyme is shown as surface, and the complex is shown as sticks.

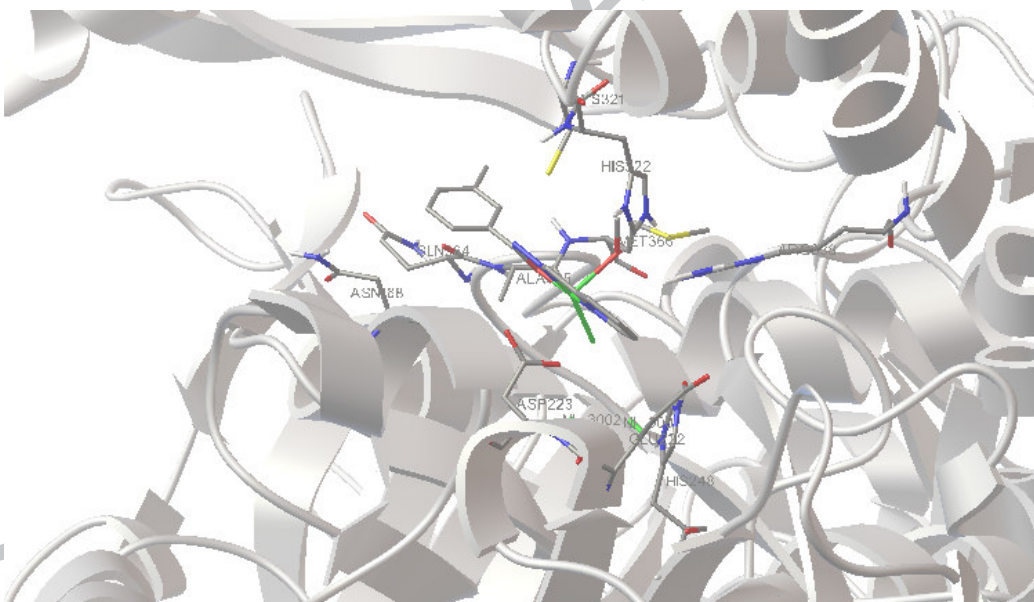


Figure 8b. Binding mode of **1** with *Jack bean* urease. The residues of the enzyme are shown as ribbon and sticks, and the complex is shown as sticks.

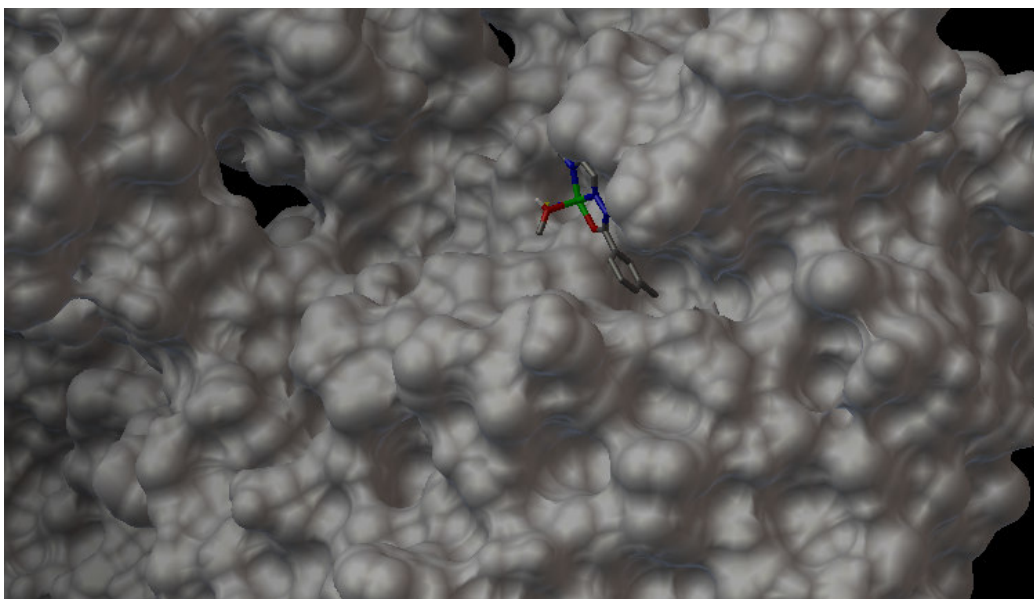


Figure 9. Binding mode of **2** with *Jack bean* urease. The enzyme is shown as surface, and the complex is shown as sticks.

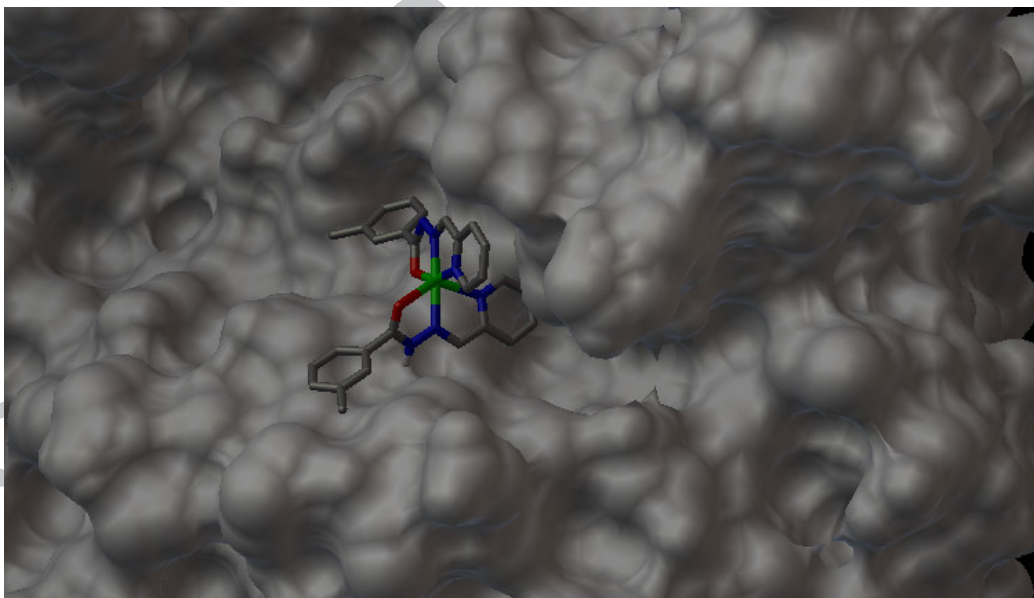


Figure 10. Binding mode of **3** with *Jack bean* urease. The enzyme is shown as surface, and the complex is shown as sticks.

Table 1 Crystal data for complexes **1**, **2** and **3**

	1	2	3
Formula	C ₁₅ H ₁₆ BrCuN ₃ O ₂	C ₁₆ H ₁₆ CuN ₄ O ₂ S	C ₂₈ H ₂₅ ClCuN ₆ O ₆
FW	413.76	391.93	640.53
Crystal shape/colour	block/blue	block/blue	block/blue
Crystal size /mm	0.31×0.27×0.27	0.27×0.26×0.23	0.27×0.23×0.23
Crystal system	Triclinic	Triclinic	Triclinic
Space group	<i>P</i> -1	<i>P</i> -1	<i>P</i> -1
<i>a</i> (Å)	7.4561(6)	8.0667(17)	8.6664(4)
<i>b</i> (Å)	8.7736(7)	9.3414(19)	11.5419(6)
<i>c</i> (Å)	12.4435(10)	13.049(2)	15.6152(8)
α (°)	87.286(2)	72.161(2)	105.408(2)
β (°)	76.280(2)	86.056(2)	96.761(2)
γ (°)	86.661(2)	66.940(2)	102.840(2)
<i>V</i> (Å ³)	788.97(11)	859.8(3)	1441.95(12)
<i>Z</i>	2	2	2
λ (MoK α) (Å)	0.71073	0.71073	0.71073
<i>T</i> (K)	298(2)	298(2)	298(2)
μ (MoK α) (cm ⁻¹)	3.926	1.407	0.903
<i>T</i> _{min}	0.3758	0.7025	0.7926
<i>T</i> _{max}	0.4171	0.7379	0.8193
Reflections/parameters	7582/204	3591/223	13738/384
Unique reflections	2920	3178	5342
Observed reflections [<i>I</i>	2455	2807	4447

$\geq 2\sigma(I)$			
Restraints	1	1	1
Goodness of fit on F^2	1.037	1.031	1.041
$R_1, wR_2 [I \geq 2\sigma(I)]$	0.0272, 0.0614	0.0314, 0.0827	0.0483, 0.1195
R_1, wR_2 (all data)	0.0367, 0.0657	0.0375, 0.0873	0.0605, 0.1295
$\Delta\rho_{\max}, \Delta\rho_{\min}, e \text{ \AA}^{-3}$	0.355, -0.288	0.425, -0.474	0.959, -0.504

ACCEPTED MANUSCRIPT

Table 2 Selected bond lengths (Å) and angles (°) for the complexes

1			
Cu1–N1	2.037(2)	Cu1–N2	1.944(2)
Cu1–O1	1.9874(19)	Cu1–O2	2.296(2)
Cu1–Br1	2.3586(4)		
N2–Cu1–O1	78.24(8)	N2–Cu1–N1	79.97(9)
O1–Cu1–N1	158.15(8)	N2–Cu1–O2	98.98(8)
O1–Cu1–O2	94.67(8)	N1–Cu1–O2	90.40(8)
N2–Cu1–Br1	162.31(7)	O1–Cu1–Br1	99.92(5)
N1–Cu1–Br1	100.30(7)	O2–Cu1–Br1	98.71(5)
2			
Cu1–N1	2.045(2)	Cu1–N2	1.9403(19)
Cu1–N4	1.913(2)	Cu1–O1	1.9949(17)
Cu1–O2	2.3245(18)		
N4–Cu1–N2	175.47(9)	N4–Cu1–O1	100.52(9)
N2–Cu1–O1	78.57(7)	N4–Cu1–N1	100.14(9)
N2–Cu1–N1	80.04(8)	O1–Cu1–N1	156.98(8)
N4–Cu1–O2	93.16(9)	N2–Cu1–O2	91.35(7)
O1–Cu1–O2	96.23(7)	N1–Cu1–O2	92.66(7)
3			
Cu – O1	2.640(2)	Cu1–O2	2.018(2)
Cu1–N1	2.255(3)	Cu1–N2	2.041(2)
Cu1–N4	2.079(3)	Cu1–N5	1.920(2)
O1–Cu1–N1	143.49(10)	O1–Cu1–N2	68.09(10)
O1–Cu1–N4	93.94(10)	O1–Cu1–N5	109.14(10)

O1-Cu1-O2	92.01(10)	N5-Cu1-O2	78.41(9)
N5-Cu1-N2	176.97(10)	O2-Cu1-N2	102.69(9)
N5-Cu1-N4	79.53(10)	O2-Cu1-N4	157.89(9)
N2-Cu1-N4	99.29(10)	N5-Cu1-N1	107.35(10)
O2-Cu1-N1	93.82(10)	N2-Cu1-N1	75.47(9)
N4-Cu1-N1	93.98(10)		

ACCEPTED MANUSCRIPT

Table 3 Hydrogen bond distances (Å) and bond angles (°) for the complexes

$D-H\cdots A$	$d(D-H)$	$d(H\cdots A)$	$d(D\cdots A)$	Angle ($D-H\cdots A$)
1				
O2-H2 \cdots N2 ⁱ	0.84(1)	2.76(3)	3.449(3)	142(4)
2				
O2-H2 \cdots N3 ⁱⁱ	0.84(1)	1.97(1)	2.800(3)	173(3)
3				
N3-H3 \cdots O5 ⁱⁱⁱ	0.90(1)	2.14(3)	2.902(4)	143(4)
C1-H1 \cdots N6 ⁱⁱ	0.930	2.43(3)	3.217(5)	142(4)
C3-H3A \cdots O4	0.930	2.48(3)	3.391(5)	166(4)
C6-H6 \cdots O5 ⁱⁱⁱ	0.930	2.52(3)	3.132(5)	124(5)
C20-H20 \cdots O1 ^{iv}	0.930	2.41(3)	3.224(5)	146(4)

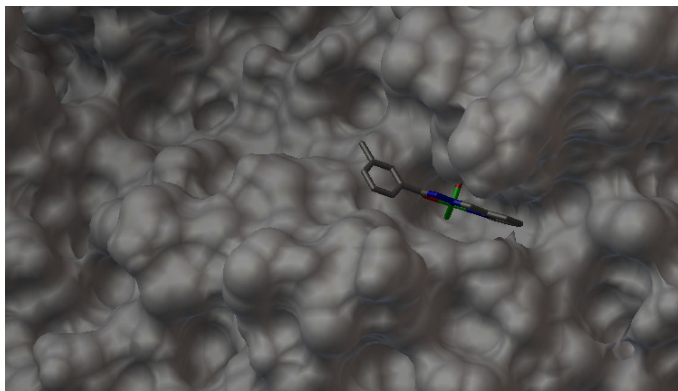
Symmetry codes: (i) $-x, 1-y, -z$; (ii) $1-x, 1-y, 1-z$; (iii) $1-x, 1-y, -z$; (iv) $-x, 1-y, 1-z$.

Table 4 Inhibition of urease by the tested materials

Tested materials	Percentage Inhibition rate [#]	IC ₅₀ (μM)
1	97.9 ± 3.8	1.46 ± 0.83
2	73.8 ± 3.1	10.8 ± 2.1
3	61.5 ± 4.0	15.4 ± 1.8
Copper perchlorate	70.2 ± 3.3	8.5 ± 1.7
Acetohydroxamic acid	64.0 ± 2.7	36.3 ± 2.5

[#]The concentration of the tested material is 12.5 μM.

Graphical abstract (picture)



ACCEPTED MANUSCRIPT

Graphical abstract (synopsis)

Three new copper(II) complexes derived from 3-methyl-*N'*-(pyridin-2-ylmethylene)benzohydrazide were prepared. Complex **1** shows effective urease inhibitory activity, with IC_{50} value of $1.46 \pm 0.83 \mu\text{M}$. Molecular docking study of the complexes with *Jack bean* urease was performed.

ACCEPTED MANUSCRIPT

▶ Three new copper(II) complexes were prepared. ▶ The complexes have been characterized by single crystal X-ray diffraction. ▶ Complex **1** has strong urease inhibitory activity. ▶ Molecular docking study of the complexes with the urease was performed.

ACCEPTED MANUSCRIPT